In Vitro Permeation and Biological Activity Of Punicalagin And Zinc (II) Across Skin and Mucous Membranes Prone To *Herpes simplex* Virus Infection

David MJ Houston[a,b], Bethan Robins[a], Joachim J Bugert[b,c], Stephen P Denyer[a,d], Charles M Heard[a*]

[a] Cardiff School of Pharmacy & Pharmaceutical Science, Cardiff University, Cardiff CF10 3NB Wales, United Kingdom

[b] Department of Microbiology & Infectious Diseases, School of Medicine, Cardiff University, Cardiff CF14 4XW Wales, United Kingdom

[c] Institute of Microbiology, Armed Forces Medical Academy, Neuherbergstraße 11, 80937 München, Germany

[d]University of Brighton, Mithras House, Lewes Road, Brighton BN2 4AT.

Abstract

Coadministration of pomegranate rind extract (PRE) and zinc (II) ions has recently been reported as a potential new topical treatment for *Herpes simplex virus* (HSV) infections. In the current work we examined the in vitro topical delivery of punicalagin (major phytochemical of PRE) and zinc from hydrogels across epithelial membranes that can become infected with HSV.

Porcine epidermal, buccal and vaginal mucous membranes were excised and mounted in Franz diffusion cells and dosed with a simple hydrogel containing PRE and zinc sulphate ($ZnSO_4$). The permeation of punicalagin and zinc were determined by HPLC and ICPMS respectively; punicalagin was also determined in the basal layers by reverse tape stripping. Receptor phases from the epidermal membrane experiment were also used to challenge HSV-1 in Vero host cells, and *ex vivo* porcine skin was used to probe COX-2 modulation.

Punicalagin and zinc permeated each of the three test membranes, with significantly greater amounts of both delivered across the epidermal membrane. The amounts of punicalagin permeating the buccal and vaginal membranes were similar, although the amount of zinc permeating the vaginal membrane was comparatively very large – it is known that zinc interacts with vaginal mucosa. The punicalagin recovered by reverse tape stripping of the epidermal, buccal and vaginal membranes gave 0.47 ± 0.016, 0.45 ± 0.052 and 0.51 ± 0.048 nM cm^{-2} respectively, and were statistically the same ($p<0.05$). A 2.5 log reduction was achieved against HSV-1 using diffusion cell receptor phase, and COX-2 expression was reduced by 64% in *ex vivo* skin after 6h.

Overall, a hydrogel containing 1.25 mg mL^{-1} PRE and 0.25 M $ZnSO_4$ was able to topically deliver both the major bioactive compound within PRE and Zn (II) across all membranes and into the site specific region of *Herpes simplex* vesicular clusters, while maintaining potentiated virucidal and anti-inflammatory properties. This novel therapeutic system therefore has potential for the topical treatment of HSV infections.

Key words: *Punica granatum L.*, pomegranate rind extract, punicalagin, zinc, virucidal, anti-inflammatory, drug delivery, *Herpes simplex* virus, skin, buccal cavity, vagina, reverse tape stripping.

1. Introduction

The pomegranate, fruit of the *Punica granatum L* tree, has been venerated since ancient times for its benefits to health (Jurenka, 2008). In recent years pomegranates have been studied more rigorously, partly in response to public preference to medicines of natural origin. The major class of phytochemicals in the pomegranate is the polyphenols and accounts for much of their antioxidant activity, flavour and colour. Extracts from the rind of the pomegranate have a large number of these polyphenols e.g. flavonoids, anthocyanins such as delphinidin, cyanidin and proanthocyanidins. Of particular interest are the hydrolysable tannins: punicalagin, punicalin, pedunicalin, as well as gallic and ellagic acid esters of glucose (Mustafa et al. 2009). The remaining phytochemicals present are organic and phenolic acids, sterols and triterpenoids, fatty acids, triglycerides, and saccharides (Seeram et al. 2005). Punicalagin, a large polyphenolic compound with a molecular mass of 1084.7, constitutes 80-85% w/w of total pomegranate tannins. Punicalagin and its degradation compounds are thought to be the main bioactive extracts present in PRE and (Seeram et al. 2005). Other bioactivities have been described for PRE and punicalagin, including antiproliferation, apoptopic and antimicrobial properties (Seeram et al. 2005; Negi and Jayaprakasha, 2003; Howell and D'Souza 2013).

Pomegranate extracts have shown antiviral effects against norovirus (Su et al. 2010), influenza virus (Haidari et al. 2009), HIV-1 (Neurath et al 2005) and poxviruses (Konowalchuk and Speirs, 1976) and it has been postulated that the interaction of plant polyphenolic compounds with the viral capsid protein may cause irreversible damage or reversible blocking of certain regions/areas of the capsid protein (Li et al. 2012). The phytochemicals of the pomegranate are concentrated in the pericarp and thus the pharmacological activity of PRE has been examined (Al-Zoreky, 2009). The combination of PRE and $FeSO_4$ was reported to produce an eleven-log reduction in the plaque forming ability of *Pseudomonas aeruginosa* and *Escherichia coli* phages within two minutes of application of an aqueous mixture at room temperature (Stewart et al. 1998). More recently, we have demonstrated that the combination of PRE and $ZnSO_4$ has potent virucidal activity against *Herpes simplex* virus-1 (HSV-1), *Herpes simplex* virus-2 (HSV-2) and aciclovir-resistant HSV-1 (Houston, 2011; Houston et al, submitted not yet accepted, a) where up to 6-log reduction was attributed to the potentiation of punicalagin, in a mechanism that is

currently under investigation. Furthermore, it was also found that PRE downregulates the short-lived endogenous inflammatory enzyme COX-2 when applied topically to *ex vivo* skin (Houston et al, submitted not yet accepted, b), which supports other reports of anti-inflammatory activity of PRE (Colombo et al. 2013). Together, these attributes indicate that coadministered PRE and zinc (II) has potential in a range of topical herpetic disorders.

HSV types 1 and 2 commonly infect skin and mucosal membranes. As there is currently no cure, individuals infected with HSV will harbour latent virus in regional nerve ganglia for the remainder of their lives. Symptoms of primary herpes include fever, malaise, tender lymphadenopathy of the head and neck, and vesicles and ulcers anywhere on oral mucosa, the pharynx, lips and perioral skin. The gingiva is typically enlarged and erythematous and lesions are painful, making it difficult to eat and drink. An important consideration for drug therapy is that the earlier the treatment is initiated, the better the outcome, especially for antiviral drugs; however, the lesions usually resolve within 10-14 days even without drug intervention. The HSV virus, which is always present in the body, tends to overcome the immune system and erupt as fluid-filled blisters that turn into sores when immune defences are run down - this is especially common during a cold viral infection. Recurring herpes has vesicles and ulcers occurring on keratinized mucosal surfaces and the lesions are grouped in a tight cluster - often a sudden prodrome of pain, tingling, or numbness precedes the onset of lesions. The frequency of recurrence varies with the individual (Pringle, 2016). Genital herpes generally causes mild symptoms; it is also possible to be infected and have no symptoms, so not everyone who is infected may be aware of the infection. When symptoms are present, they consist of typically painful blisters around the genital or rectal area. The blisters break open, form ulcers, and take 2 to 4 weeks to heal. With the first outbreak of genital herpes, a person may also experience flu-like symptoms including fever, body aches, and swollen lymph nodes. Immediately prior to an outbreak, there may be an itching, burning, or tingling sensation of the skin. In women, genital herpes usually causes blistering lesions on the vulva and around the vaginal opening that progress to ulcer formation. The infection spreads to involve the cervix in most cases, leading to cervicitis (inflammation of the cervix). In some cases cervicitis may be the only sign of genital herpes infection. Infection and inflammation

of the urethra accompanies the infection in some women, leading to pain on urination. After the initial infection, a person may or may not have outbreaks later in life.

The current work thus investigated the in vitro topical delivery of PRE and $ZnSO_4$ and its breadth of applicability to the various anatomical regions prone to infection with HSV-1 and HSV-2. *Herpes simplex* labialis lesions (cold sores) mainly affect the perioral region (in which case normal skin can be used as a model for determining penetration), however, they also occur on the lips and in the mucous membranes of the buccal cavity, such as inner cheeks and gums (Pringle, 2016). Anogenital infections of HSV can involve the areas of normal skin or mucous membranes, or both. Depending on the progression of the lesion, the precise location of the viral load can vary from within the skin to near or on the surface (Salameh et al. 2012). Here, we used porcine skin, buccal and vaginal membranes excised by blunt dissection which, being intact, would represent the minimum amounts of permeants delivered into these membranes. In the case of advanced lesions the skin barrier would compromised and so the amounts deliverable would be expected to be substantially greater, particularly given the hydrophilic nature of the actives and the hydrated state of the buccal and vaginal mucosal membranes.

The objective of this work was thus to determine the *in vitro or ex vivo* permeation of punicalagin and zinc (II) using models for HSV-1 and HSV-2 vesicular specific sites, from topically applied hydrogel formulations containing PRE and $ZnSO_4$ and to determine if virucidal and anti-inflammatory activities are retained following membrane permeation.

2. Materials and methods

2.1. Materials

Pomegranates were obtained from a local supermarket and were of Spanish origin. Hydroxypropylmethyl cellulose (Methocel 856N) was a gift from The Dow Chemical Company, MI, USA. Zinc sulphate ($ZnSO_4$), Dulbecco's modified eagle medium (DMEM), potassium hydrogen phthalate, bovine serum albumen (BSA), bromophenol blue (99%, UV-VIS), dimethyl sulfoxide (DMSO, 99%), gentamycin sulfate, glycerol (99%), glycine (99%), *N,N,N',N'*-tetramethyl-ethylenediamine

(TEMED, 99%), positive control lysate for COX-2 (Human cells-13 lysate, 250 μg in 0.1 mL), sodium bicarbonate ($NaHCO_3$, 99%), sodium chloride (NaCl, 99.9%), sodium dodecyl sulphate (SDS), tris (hydroxymethyl)methylamine (Tris base, 99.8%), Thermo Scientific SuperSignal® west dura extended duration substrate, filter paper QL100 (equivalent to Whatman Grade 1), nitrocellulose transfer membrane (Whatman Protran® BA85 with pore size of 0.45 μm), trifluoroacetic acid (TFA) and all other solvents were of analytical grade or equivalent were obtained from Fisher Scientific (Loughborough, UK). Aprotinin (≥98%), dithiothreitol (DTT, 1 M in water), ethylene diamine tetraacetic acid (EDTA, 98%), Hanks' balanced salt buffer (HBSB), leupeptin hydrochloride (≥70%), monoclonal anti-β-actin antibody produced in mouse (clone AC-74, ascites fluid, A 5316), [4-(2-hydroxyethyl)-1-piperazineethanesulfonic acid] (HEPES, ≥99.5%), phenylmethylsulphonyl fluoride (PMSF, ≥99%), phosphate buffer solution (PBS, pH 7.4), polyoxyethylene-sorbitan monolaurate (Tween® 20), ponceau S, RIPA buffer and punicalagin were all purchased from Sigma-Aldrich (Poole, UK). Cyclooxygenase-2 antibody (COX-2, #4842), anti-rabbit immunoglobulins (IgG) horseradish-peroxidase (HRP)-linked antibodies and positive controls for COX-2 (RAW 264.7 cells lysate, untreated or LPS treated) by Cell Signaling Technology were purchased from New England BioLabs Ltd. (Hitchin, UK). MXB autoradiography film (blue sensitive: 18 × 24 cm^2) was obtained from Genetic Research Instrumentation (Braintree, UK). Full range Rainbow® recombinant protein molecular weight marker (12 - 225 kDa) was purchased from GE Healthcare Life Sciences (Little Chalfont, UK) and Bio-Rad protein assay reagent from Bio-Rad Laboratories GmbH (Munich, Germany). Freshly excised porcine ears, cheeks and vaginas were obtained from a local abattoir and immersed in iced HBSB solution upon excision, and used within 1 h of slaughtering.

2.2. Preparation of Pomegranate Rind Extract (PRE)

Six fresh pomegranates were peeled; the rinds cut into thin strips approximately 2 cm in length, blended in deionised H_2O (25% w/v) and boiled for approximately 10 min. The crude suspension was then transferred into centrifuge tubes and centrifuged at 10,400g at 4□C for 30 min using a Beckman Coulter Avanti J25 Ultracentrifuge and vacuum filtered through a Whatman 0.45□m nylon

membrane filter. The solution was then freeze-dried, occluded from light and stored at -20□C until required. The punicalagin concentration of each extract was analysed, and consisted of 20% w/w of PRE. The PRE was reconstituted by adding 2 mg to 10 mL of pH 4.5 phthalate buffer. The solution was sonicated for 10 min at 50-60 Hz and once fully dissolved, filtered through a 0.45 □m Millex®-FG syringe driven filter unit and stored at -20°C until further use.

2.3. Hydroxypropyl Methylcellulose (HPMC) Hydrogel

Using the 'hot/cold' technique, 2.5g HPMC (Methocel 856N) was added to 40 mL pH 4.5 phthalate buffer at 80 °C with constant stirring until all particles are thoroughly wetted. 60 mL cold or iced deionised H_2O was then added to the solution with constant agitation for 30 min. This enabled the hydration of the powder and the increase in the viscosity of the resulting hydrogel, which was then cooled to 4°C. PRE and $ZnSO_4$ were added to 60 ml of cold phthalate buffer: hydrogel H1 0.5 mg mL^{-1} PRE, 0.1 M $ZnSO_4$; H2 1.25 mg mL^{-1} PRE, 0.25 M $ZnSO_4$; blank contained neither PRE nor $ZnSO_4$ (Table 1). Agitation of the hydrogel continued for 30 min after the addition of the cooled water to guarantee a uniform and evenly dispersed hydrogel. All formulations were refrigerated for a minimum of four hours after agitation so that a uniform hydrogel was formed (Dodov et al. 2005). It had previously been found that HPMC yielded gels with good tactile and rheological properties (Houston, 2011).

2.4. Preparation of Porcine Membranes

Heat separated epidermis was used to model drug delivery to HSV-1 and -2 vesicular clusters which form in the early stages of a HSV or cold sore lesion formation, where the skin and barrier function are still essentially intact, and could also represent surrounding non-labial regions either of the mouth or vagina.

The freshly excised porcine ears were gently washed under cool running water and full thickness skin was removed from the dorsal cartilage by blunt dissection, using a scalpel. The skin was further sectioned into 2 cm^2 squares and immersed in water at 55°C for 1 min (Kligman and Christophers, 1963) then used straight away.

For the COX-2 determinations (Section 2.10), *ex vivo* full thickness skin was carefully liberated from cleaned, shaved ears, whilst being bathed continually with HBSB (Houston et al. submitted not yet accepted, b).

Heat separated buccal membrane was used as HSV-1 and -2 most commonly transverse the trigeminal nerve which enables the virus to present not only on the prolabium but also within the buccal cavity, it was important to determine the delivery of both punicalagin and zinc across the buccal mucosa. Porcine cheeks were collected from a local abattoir as soon as possible after slaughter, then transported to the lab immersed in iced buffered HBSB and application of test materials began within an hour of excision. The buccal membrane was carefully excised from the underlying tissues using a scalpel until only the top mucosal membrane remained, this was sectioned into 2 cm^2 pieces and immersed in water at 55°C for 1 min, then used immediately.

Porcine vaginal membrane was used to model the presentation of HSV-1 and -2 vesicular clusters within and around the vaginal cavity soft tissue in female *Herpes simplex* infection. Porcine vaginas were collected from a local abattoir as soon as possible after slaughter, then transported to the lab immersed in iced buffered HBSB and application of test materials began within an hour of excision. Excess fat and muscle was cut away from the porcine inner vaginal wall via scalpel dissection. The vaginal cavity was opened by cutting one vaginal wall from the vaginal opening to the cervix. The vaginal mucosal membrane was then trimmed using a scalpel until only the mucosal membrane remained, this was sectioned into 2 cm^2 pieces and used immediately.

2.5. In Vitro Membrane Permeation Determination

All-glass Franz diffusion cells (FDC) were used with nominal diffusional area of 1 cm diameter (0.88 cm^2) and nominal receptor phase volume of 3 mL. The relevant membrane was mounted epithelium-uppermost on the lightly pre-greased flanges of the receptor. The donor chamber was placed on top of the membrane and clamped into position. A micro-stirrer bar was added to the receptor compartment, filled with deionised H_2O and the sampling arm capped. The cells were placed on a

multiple stirrer plate in a thermostatically controlled water bath set at 37°C for 15 min to allow the temperature to reach equilibrium. An infinite dose of 300 mg aliquot of hydrogel H1, H2 and blank was applied (without stirring due to the fragility of the buccal and vaginal membranes), thus allowing determination of maximal levels of drug delivery. At specific timepoints the receptor fluids were removed using a sterile pipette and stored in 10 mL glass vials until further use; the receptor chamber was then refilled with deionised H_2O.

2.6. Reverse Tape Stripping

Tape stripping is typically performed to determine depth profiles for drug penetration into biological membranes, mainly (Williams, 2003). Here we took a different approach in the knowledge that replicating HSV infects the viable epidermis, thus the amount of permeant localised within the basal layer is of particular interest. Thus instead of stripping the outer layer of the membrane, which is in contact with the donor phase, the inner side (which is in contact with the receptor fluid) was the starting point of the stripping procedure.

The membrane was removed from the FDC after 24 h using forceps and dabbed clean of formulation carefully and trimmed to the area of application. A drop of cyanoacrylate adhesive was applied to a ceramic tile, the membrane was placed on the adhesive, donor phase side downwards. Regular adhesive tape strips (Sellotape) were then gently pressed onto the membrane and the tape was then carefully removed using forceps, placed in an Eppendorf vial containing 2 mL of methanol and rocked overnight. The tape was removed from the vial and the methanol evaporated under vacuum before 2 mL of deionised H_2O was added. To allow a comparative determination of the levels of actives in the basal layer areas of the 3 test membranes, reverse tape stripping was conducted after 24 h.

2.7. Analysis of Punicalagin by HPLC

In this work punicalagin was used as marker for PRE – punicalagin is the tannin in highest concentration in PRE and has previously been shown to exert the

greatest effect on *Herpes simplex* virus (Houston, 2011; Houston et al, unpublished a). The analysis was performed using an Agilent series 1100 HPLC system fitted with a Phenomenex Gemini NX C18 110A 250 x 2.6 mm column. Gradient elution was used, involving A = methanol with 0.1% trifluoroacetic acid (TFA) and B = deionised H_2O with 0.1% TFA: 0 min A 5% B 95%, 15 min A 20% B 80%, 30 min A 60% B 40%, 40 min A 60% B 40%. Injection volume was 20 μL and detection was by UV at 258nm. Punicalagin naturally occurs as a pair of isomers (anomers), α and β, in the ratio of 1:2 (Figure 1). Aqueous solutions of punicalagin standard were analysed over a range of concentrations and the resulting calibration curves of the α and β anomers (Figure 1) were used to determine total punicalagin levels by summation of the areas of the two corresponding peaks in the test sample chromatograms.

2.8. Analysis of Zinc by Inductively Coupled Plasma Mass Spectrometry (ICPMS)

The levels of zinc permeating the skin were determined by ICPMS analysis (Li et al. 2012) using a Thermo Elemental X Series 2 ICP-MS system equipped with a Plasma Screen. Analysis was performed using ^{66}Zn as the analytical mass. Calibration was carried out using standard solutions prepared from single element stock standards. Periodic checks for accuracy were performed by analysis of a solution of the international rock standard JB1a as an unknown - this standard was prepared by digesting a sample in HF/HNO_3 and then HNO_3. Data were plotted as cumulative permeation vs time. It was necessary to pool the repeat samples and so replicate data were not obtained.

2.9. Virucidal Activity of Receptor Phase Against HSV-1

Here we determined whether the receptor phases retained virucidal activity against HSV-1 following termination of the permeation experiment, using Vero host cells. The method is described in detail elsewhere (Houston, 2011; Houston et al. submitted not yet accepted a) and briefly involved HSV-1 incubation with the test material for 30 min before serial dilution and plating onto 24 well-plate of confluent Vero cells for a 3 day incubation, at which point the plaques were counted and results calculated a log-reduction.

2.10. Western Blot Analysis of COX-2

Our previous work has demonstrated that constituent phytochemicals of topically applied PRE penetrate *ex vivo* skin and result in the downregulation of COX-2 expression (Houston et al. submitted not yet accepted b) - here we tested the hypothesis that these phytochemicals as permeants in the receptor phase retain this previously observed antiinflammatory activity. In a departure from the method outlined in section 2.5, full thickness, *ex vivo* porcine membranes were used and the receptor phase was HBSB to prolong viability. Following termination of the penetration experiment (6 h) the membranes were retrieved, cleaned and homogenised in RIPA buffer using a probe homogeniser. The relative levels of inflammation marker COX-2 was carried out by Western blotting analysis using β-actin as the loading control, and followed a previously reported method (Houston 2011; Abu Samah and Heard, 2014)

2.11. Data Processing

Statistical tests were performed using Instat 3 for Macintosh. A one way analysis of variance test was applied with a confidence interval of 95%, and a *p* value of <0.05 was considered significant. If values were found to be of significance a Turkey-Kramer multiple comparison test was applied.

3. Results and discussion

3.1. Permeation of Punicalagin and Zinc (II) across Epidermal Membranes

Figure 2 depicts the permeation profiles of punicalagin across heat-separated epidermis from hydrogels H1 and H2; a blank gel was run as a control. Results show that the permeation of punicalagin from H2 was higher than H1 due to the higher concentration and therefore higher chemical potential within this gel. Thus a greater release and permeation of punicalagin from the hydrogel matrix would be expected. Permeation of punicalagin from H2 was detectable within 0.5 h (1 nM cm^{-2}).

However, Table 1 shows that punicalagin permeation after 6h was approximately 4x more from H2 compared to H1 (4.2 ± 0.15 vs 0.96 ± 0.36 nM cm^{-2}); the same difference was maintained after 12h (5.4 ± 0.35 vs 1.4 ± 0.36 nM cm^{-2}). This was surprising given the 2.5x difference in PRE loading between the two hydrogels.

Figure 3 shows the permeation of zinc across the epidermal membranes from hydrogels H1 and H2 and blank. It can be seen that zinc was detectable in the receptor phase after application of the control blank gel and was due to a leaching of zinc which is naturally found in the skin. Table 1 shows that zinc permeation after 6h was approximately 2.3x more from H2 compared to H1 (520 vs 220 ± nM cm^{-2}); the same difference was maintained after 12h (630 vs 260 nM cm^{-2}). This differential was in line with 2.5x difference in $ZnSO_4$ loading between the two hydrogels.

Together, Figures 2 and 3 demonstrate that both punicalagin and zinc permeated the epidermis following the topical application of hydrogels H1 and H2. This is despite the fact that punicalagin is a large molecule with a MW of 1084.7, whereas the optimum for skin permeation is around 350, and the purported general impermeability of skin to small polar molecules such as Zn^{2+}. In the formulations zinc was in present excess over punicalagin and this was reflected in the permeation data show there was a molar excess of permeated zinc/punicalagin which was greater for H1 (approx. x207) than H2 (approx. x120).

3.2. Localisation of Punicalagin in Heat Separated Epidermis Basal Layer Region

Epidermal membranes were recovered at 24 h and subjected to reverse tape stripping, with three strips taken on each occasion. Figure 4 shows that from both hydrogels applied, punicalagin localised at significantly higher concentration within the lowest strip, i.e. the basal layer ($p<0.05$). The second and third tape strip revealed a significantly lower level of punicalagin delivery by both gels, towards the skin surface. The fact that localisation from hydrogels H1 and H2 were the same indicates in both cases the attainment of membrane saturation ie no capacity to bind further molecules. The effect on binding of the probable presence of other constituents within PRE is unknown. Overall, these data confirm that punicalagin was successfully delivered to the skin site where HSV-1 and -2 vesicular clusters occur.

3.3. Virucidal Activity of Franz Diffusion Cell Receptor Phases Against HSV-1

The receptor phases were recovered after 24h and used to challenge HSV-1 infected host cells, and the HSV-1 virucidal data are shown in Figure 5. When the skin was dosed with blank hydrogel the receptor phase from the blank hydrogel showed negligible log reduction of viral load. However, the receptor phase from hydrogel H2 resulted in a significant 2.57 ± 0.36 log reduction of HSV-1 plaque-forming units (pfus). This demonstrates the successful delivery of both punicalagin and Zn II across the heat separated epidermis in the concentration ranges of both compounds that provide virucidal activity (Houston et al. submitted not yet accepted a)

3.4. Anti-inflammatory Activity

To verify that the permeation of punicalagin from hydrogel H2 retained anti-inflammatory activity as found previously (Houston et al. submitted not yet accepted b), the relative levels of COX-2 were determined by Western blotting analysis of *ex vivo* skin. Hydrogel H2 and blank control were applied to *ex vivo* full thickness porcine skin within a Franz diffusion cell for 6 h. After this time SDS-PAGE and Western blotting were carried out for COX-2, as an inflammatory marker, using β-Actin as ubiquitous protein loading control. Figure 6 shows the bands produced by Western blot analysis for COX-2 expression at ~ 72 kDa and the protein loading control of β-actin at ~42 kDa. Densitometric analysis of the bands for COX-2 were normalised using β-actin, levels of COX-2 expression in the control were arbitrarily assigned a value of 100%. The application of hydrogel H2 caused the statistically significant reduction of COX-2 expression by 67.69 ± 3.93% (p<0.01), and demonstrates the permeated compounds were able to modulate the arachidonic acid inflammation pathway by downregulating COX-2 production. The reduction of COX-2 following the application of the hydrogel H2 was statistically the same as that observed when (1 mg mL^{-1}) PRE was dosed – data not shown.

3.5. Permeation of Punicalagin and Zinc II Across Buccal Membranes

Buccal membrane was used as a model for the presentation of HSV-1 lesions within mucous membranes of the buccal cavity. Figure 7 shows the permeation of

punicalagin from hydrogel H2 across buccal membrane compared to that across epidermal and vaginal membranes. Permeation of punicalagin was detectable within 0.5 h (1 nM cm^{-2}). After 6h the permeation of punicalagin across buccal membrane was approximately half that across epidermal membrane (1.95 ± 0.5 vs 4.2 ± 0.15 nM cm^{-2} respectively). After 12 h, the differential was the same (2.6 ± 0.7 vs 5.4 ± 0.35 nM cm^{-2} respectively).

Pooled skin extracts analysed by ICPMS revealed that the amount of zinc leached from the buccal membrane after application of blank hydrogel was much lower concentration in comparison to epidermal membrane (Table 1). Figure 8 shows the permeation of zinc across the buccal membrane from H2, after blank subtraction in comparison with that across epidermal and vaginal membranes. Table 1 shows that after 6h the permeation of zinc across buccal membrane was ~ one quarter of that across epidermal membrane (125 vs 520 nM cm^{-2}). After 12 h, the differential was similar at 3.5x (180 vs 630 nM cm^{-2} respectively). The permeation of profile of zinc over the 24 h period is similar to that through HSE - a plateau was observed after 1 h, maintained up to 12 h and tailing off.

3.6. Permeation of Punicalagin and Zinc II Across Vaginal Membranes

The permeation of punicalagin from hydrogel H2 across the vaginal membrane, along with that across epidermal and buccal membranes, is illustrated in Figure 7. Permeation of punicalagin was detectable within 0.5 h (0.7 nM cm^{-2}). The permeation of punicalagin across vaginal membrane was lower than across buccal membrane, although not statistically significant at the 95% level. Table 1 shows that at 6 h the amounts permeated were 1.45 ± 0.25 vs 1.95 ± 0.5 nM cm^{-2} respectively ($p>0.05$); at 12 h the amounts permeated were 1.7 ± 0.3 vs 2.6 ± 0.7 nM cm^{-2} respectively ($p>0.05$). However, as with buccal membranes the permeation of punicalagin across vaginal membranes was statistically lower than across epidermal membranes

The permeation of zinc across the vaginal mucosal membrane from H2 after blank subtraction is shown in Figure 8. The leaching of zinc from the vaginal membranes after application blank hydrogel was not significantly different ($p>0.05$) to that leached from the buccal membrane (not shown), but was a lot less than that

from the epidermal membrane. However, the permeation profile in Figure 8 reveals that zinc permeated to a much greater extent compared to both epidermal and buccal membranes. Although zinc salts have been reported to inactivate HSV-1 isolates (Arens and Travis, 2000) zinc salt solutions have also been reported to cause sloughing of sheets of vaginal epithelial cells (Bourne et al. 2005). Although this provides for increased permeation of biocide, it also has the potential to cause damage to the vaginal mucosal membrane that might increase susceptibility to secondary infections at a later time.

3.7. Comparison of Reverse Tape Stripping Epidermal, Buccal and Vaginal Membranes after 24 h Application of H2

Figure 9 shows a comparison of the punicalagin recovered by reverse tape stripping of the epidermal, buccal and vaginal membranes. The values, 0.47 ± 0.016, 0.45 ± 0.052 and 0.51 ± 0.048 nM cm^{-2} respectively, were in close agreement and statistically the same ($p<0.05$). The results indicate that punicalagin is being delivered similarly through all three membranes to the target site where vesicular clusters occur.

4. Conclusions

This work has demonstrated that a simple hydrogel based upon 2.5% HPMC, 1.25 mg mL^{-1} PRE and 0.25 M $ZnSO_4$ in pH4.5 phthalate buffer was able to topically deliver the major bioactive compound within PRE and Zn (II) across membranes and to the site specific regions of *Herpes simplex* vesicular clusters. This is despite the relatively large MW of punicalagin and small charged nature of zinc ions which would conventionally suggest their relatively low permeability. In doing so, the potentiated virucidal and anti-inflammatory activities observed previously were maintained. In summary, a novel therapeutic system for the topical treatment of HSV-1 and HSV-2 lesions is proposed based on the pomegranate in combination with Zn (II).

Acknowledgements

This work was financially supported by Welsh Assembly Government grant RFSSA07-03-013.

REFERENCES

Abu Samah, N.H., Heard, C.M., 2014. The effects of topically applied polyNIPAM-based nanogels and their monomers on skin cyclooxygenase, ex vivo. Nanotoxicology 8, 100-106.

Al-Zoreky, N.S., 2009. Antimicrobial activity of pomegranate (*Punica granatum L.*) fruit peels. International Journal of Food Microbiology 134, 244-48.

Arens, M., Travis, S., 2000. Zinc salts inactivate clinical isolates of herpes simplex virus in vitro. J. Clin. Microbiol. 38, 1758-1762.

Bourne, N., Stegall, R., Montano, R., Meador, M.,, Stanberry, L.R., Milligan, G.N., 2005. Efficacy and toxicity of zinc salts as candidate topical microbicides against vaginal herpes simplex virus type 2 infection. Antimicrobial Agents and Chemotherapy Antimicrob. 49, 1181-1183.

Colombo, E., Sangiovanni, E., Dell'Agli, M., 2013. A review on the anti-inflammatory activity of pomegranate in the gastrointestinal tract. Evidence-Based Complementary and Alternative Medicine, Article ID 247145.

Dodov, M.G., Goracinova, K., Simonoska, M., Trajkovic-Jolevska, S., Ribarska, J.T., Mitevska, M.D., 2005. Formulation and evaluation of diazepam hydrogel for rectal administration. Acta Pharm. 55, 251-261.

Haidari, M., Ali, M., Casscells, S.W., Madjid, M., 2009. Pomegranate (*Punica granatum*) purified polyphenol extract inhibits influenza virus and has a synergistic effect with oseltamivir. Phytomedicine 16, 1127–1136.

Houston, D.M.J., 2011. Towards a nanomedicine-based broadspectrum topical virucidal therapeutic system. PhD thesis, Cardiff University.

Houston, D.M.J., Bugert, J.J., Denyer, S.P., Heard, C.M. Submitted not yet accepted, a. Potentiated virucidal and anti-viral activity of pomegranate rind extract and zinc II ions against *Herpes simplex* virus and aciclor-resistant *Herpes simplex* virus.

Houston, D.M.J., Bugert, J.J., Denyer, S.P., Heard, C.M. Submitted not yet accepted, b. Probing the ex vivo anti-inflammatory properties and cytotoxicity of topically applied pomegranate rind extract, total pomegranate tannins and zinc sulphate.

Howell, A.B., D'Souza, D.H., 2013. The pomegranate: effects on bacteria and viruses that influence human health. Evidence-Based Complementary and Alternative Medicine. Article ID 606212.

Jurenka, J., 2008. Therapeutic applications of pomegranate (Punica granatum L.): A Review. Alternative Medicine Review 13, 128-144.

Kligman, A.M., Christophers, E., 1963. Preparation of isolated sheets of human stratum corneum. Archives of Dermatology 88, 702-705.

Konowalchuk, J., Speirs, J.I., 1976. Antiviral activity of fruit extracts. Journal of Food Science 41, 1013–1017.

Li, D., Baert, L., Xia, M., Zhong, W., Jiang, X., Uyttendaele, M., 2012. Effects of a variety of food extracts and juices on the specific binding ability of norovirus GII. 4 P particles. Journal of Food Protection 75, 1350–1354.

Li, G., Brockman, J.D., Lin, S.W., Abnet, C.C., Schell, L.A., Robertson, J.D., 2012. Measurement of the trace elements Cu, Zn, Fe, and Mg and the ultratrace elements Cd, Co, Mn, and Pb in limited quantity human plasma and serum samples by inductively coupled plasma-mass spectrometry. American Journal of Analytical Chemistry 3, 646-650.

Mustafa, C., Yasar, H., Gokhan, D., 2009. Classification of eight pomegranate juices based on antioxidant capacity measured by four methods. Food Chemistry 112, 721-726.

Negi, P.S., Jayaprakasha, G.K., 2003. Antioxidant and antibacterial activities of Punica granatum peel extracts. Food Microbiology and Safety 68, 1136-1553.

Neurath, R., Strick, N., Li, Y.Y., Debnath, A.K., 2005. Punica granatum (pomegranate) juice provides an HIV-1 entry inhibitor and candidate topical microbicide. In Natural Products and Molecular Therapy, G. J. Kotwal and D. K. Lahiri, Eds., 1056: 311–327, New York Academy of Sciences.

Pringle, C.R., 2016. Herpes Simplex Virus Infections. https://www.merckmanuals.com/home/infections/viral-infections/herpes-simplex-virus-infections

Salameh, S., Sheth, U., Shukla, D., 2012. Early events in herpes simplex virus lifecycle with implications for an infection of lifetime. Open Virol J. 6, 1–6.

Seeram, N.P., Adams, L.S., Henning, S.M., Niu, Y., Zhang, Y., Nair, M.G., Heber, D., 2005. In vitro antiproliferative, apoptotic and antioxidant activities of punicalagin, ellagic acid and a total pomegranate tannin extract are enhanced in combination with other polyphenols as found in pomegranate juice. Nutritional Biochemistry 16, 360-367

Stewart, G.S.A.B., Jassim, S.A., Denyer, S.P., 1998. The specific and sensitive detection of bacterial pathogens within 4 h using bacteriophage amplification. Applied Microbiology 84, 777-783.

Su, X., Sangster, M.Y., D'Souza, D.H., 2010. In vitro effects of pomegranate juice and pomegranate polyphenols on foodborne viral surrogates. Foodborne Pathogens and Disease 7, 1473–1479.

Williams, A.C., 2003. Transdermal and Topical Drug Delivery, from Theory to Clinical Practice. Pharmaceutical Press, London.

Figure legends

Figure 1 HPLC chromatogram of punicalagin showing peaks for α and β anomers in 1:2 ratio and resulting calibration curves.

Figure 2 Cumulative permeation of punicalagin across epidermis after application of 1 mL hydrogels H1, H2 and blank control (mean ± SD, n= 4).

Figure 3 Cumulative permeation of zinc across epidermis after of 1 mL hydrogels H1, H2 and blank control (mean ± SD, n= 4).

Figure 4 Reverse tape stripping: punicalagin recovered after 24h by reverse tape stripping three times epidermal membranes (1 being lowest) dosed with formulation, for each pair of bars: left = H1 and right = H2 (mean ± SD, n= 4).

Figure 5 Virucidal log reduction of HSV-1 after the incubation with receptor phase following 24 h application of H1 and H2 to epidermis, blank was negligible (mean ± SD, n= 4).

Figure 6 Modulation of COX-2 protein expression following dosing of ex vivo skin with receptor phase following 6h application of H2 and phthalate buffer as a control to ex vivo skin. Protein was extracted and 30 µg was loaded and separated through SDS-PAGE. The histogram represents numerical data of COX-2 normalised using β-actin. Levels in the control were arbitrarily assigned a value of 100% (mean ± SD, n= 4).

Figure 7 Permeation profile of punicalagin from H2 and blank across the epidermal, buccal and vaginal membranes (mean ± SD, n= 4).

Figure 8 Permeation profiles for zinc across epidermal, buccal and vaginal membranes after application of H2 (singlicate determination).

Figure 9 Reverse tape stripping: comparison of punicalagin recovered from lowest reverse tape strip after 24 h application of hydrogel H2 to epidermal, buccal and vaginal membranes (mean ± SD, n= 4).

Table 1: Cumulative permeation of punicalagin (mean ± SD, n= 4) and zinc (n=1) from 2.5% HPMC hydrogels across epidermal, buccal and vaginal membranes. H2: PRE 1.25 mg mL^{-1}, $ZnSO_4$ 0.25 M; H1 PRE 0.5 mg mL^{-1}, $ZnSO_4$ 0.1 M; blank PRE 0, $ZnSO_4$ 0.

Membrane	Hydrogel	Punicalagin 6h nM cm^{-2}	Zn 6h nM cm^{-2}	Punicalagin 12h nM cm^{-2}	Zn 12h nM cm^{-2}
Epidermal	H2	4.2 ± 0.15	520	5.4 ± 0.35	630
	H1	0.96 ± 0.36	220	1.4 ± 0.36	260
	blank	-	85	-	90
Buccal	H2	1.95 ± 0.5	125	2.6 ± 0.7	180
	blank	-	10	-	13
Vaginal	H2	1.45 ± 0.25	22 x 10^3	1.7 ± 0.3	29 x 10^3
	blank	-	0.5	-	0.5

Figure 1

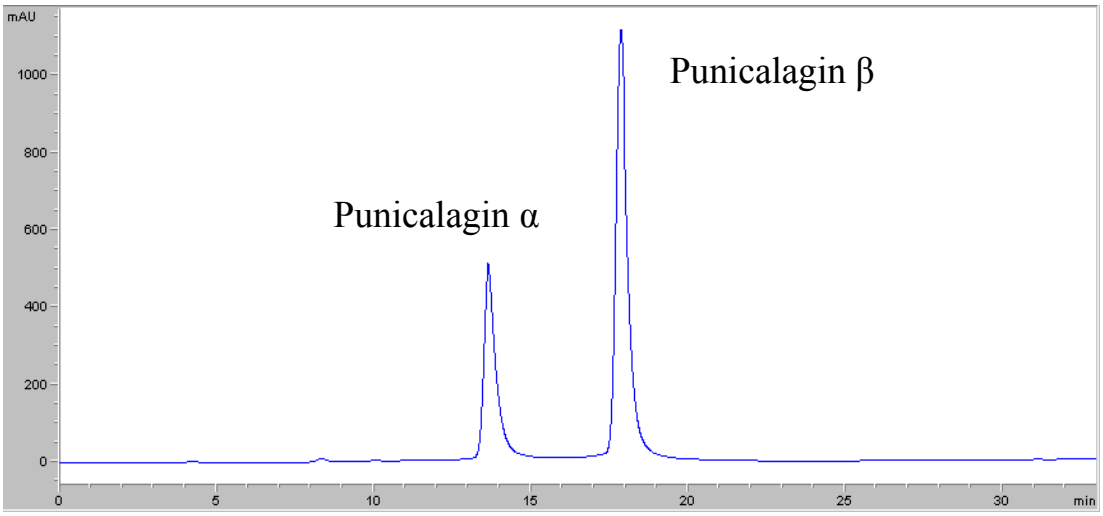
mAU
1000
800
600
400
200
0
Punicalagin β
Punicalagin α
0
5
10
15
20
25
30
min

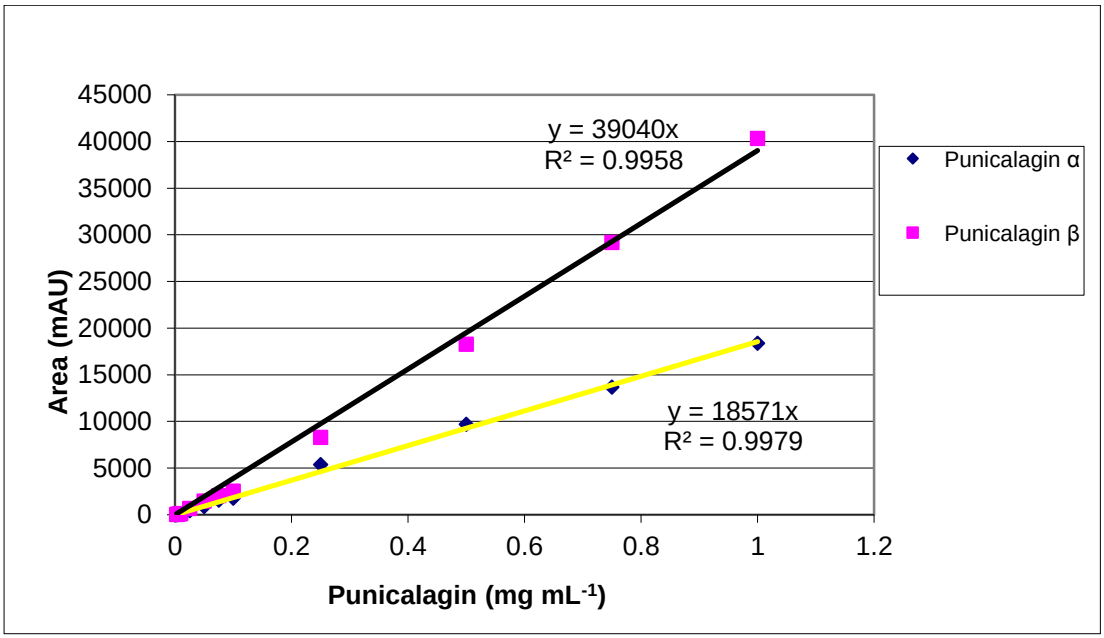
45000
40000
35000
30000
25000
20000
15000
10000
5000
0
Area (mAU)
y = 39040x
R² = 0.9958
y = 18571x
R² = 0.9979
Punicalagin α
Punicalagin β
0
0.2
0.4
0.6
0.8
1
1.2
Punicalagin (mg mL-1)

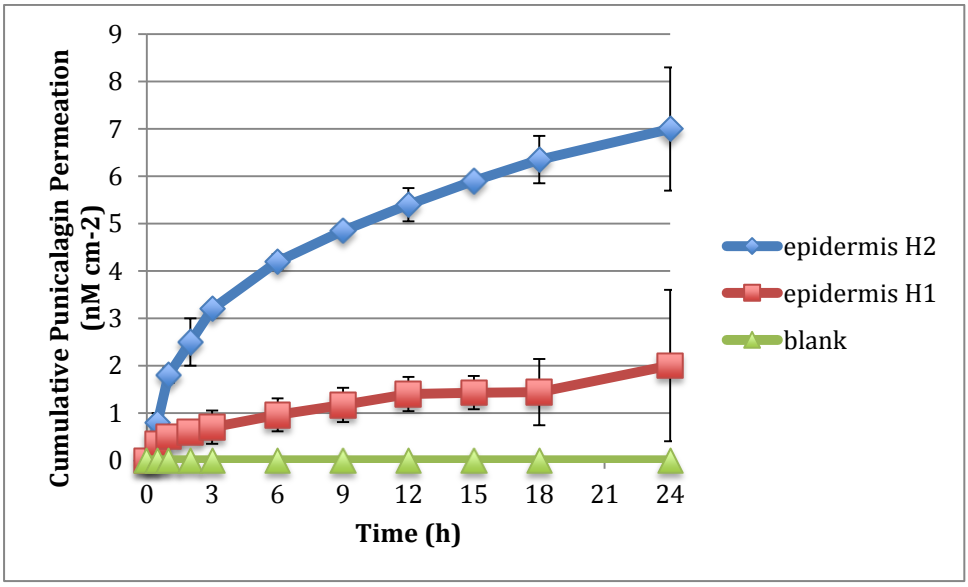
Cumulative Punicalagin Permeation (nM cm-2)
9
8
7
6
5
4
3
2
1
0
0
3
6
9
12
15
18
21
24
Time (h)
epidermis H2
epidermis H1
blank

Figure 2

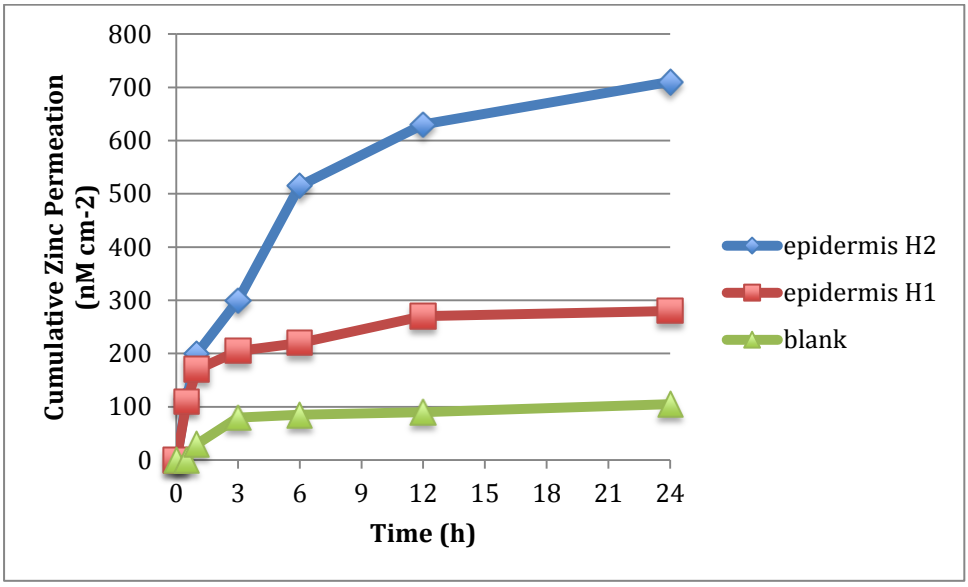
Cumulative Zinc Permeation (nM cm-2)
800
700
600
500
400
300
200
100
0
0
3
6
9
12
15
18
21
24
Time (h)
epidermis H2
epidermis H1
blank

Figure 3

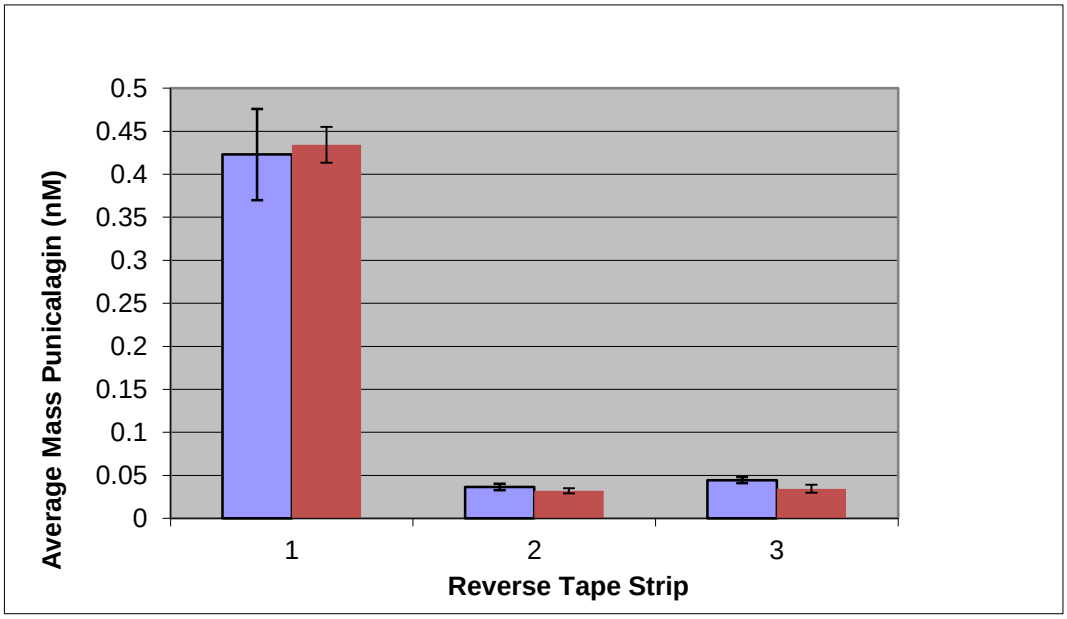
Average Mass Punicalagin (nM)
0.5
0.45
0.4
0.35
0.3
0.25
0.2
0.15
0.1
0.05
0
1
2
3
Reverse Tape Strip

Figure 4

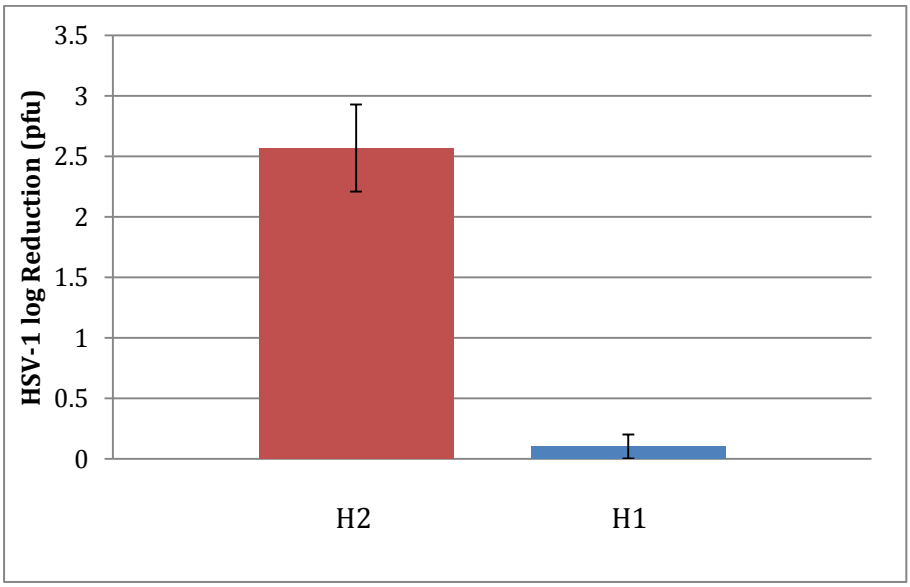

Figure 5

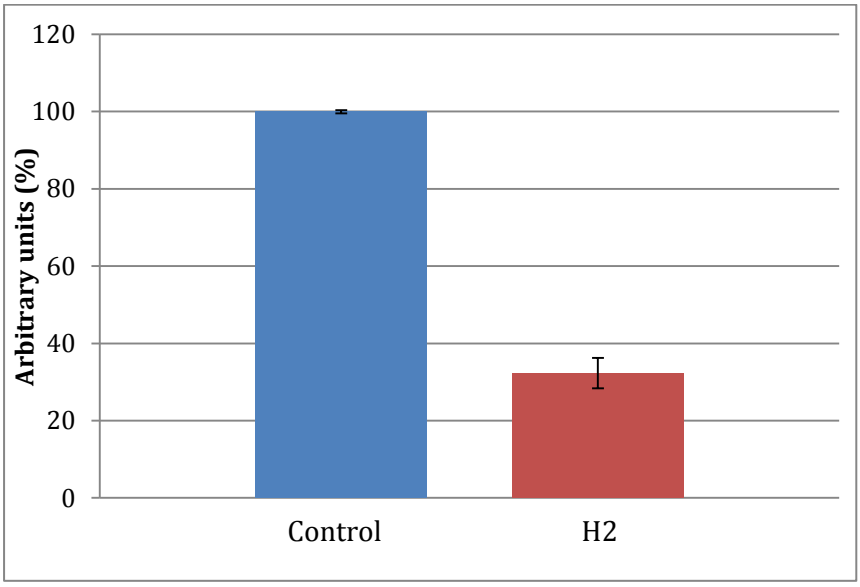
120
100
80
60
40
20
0
Arbitrary units (%)
Control
H2

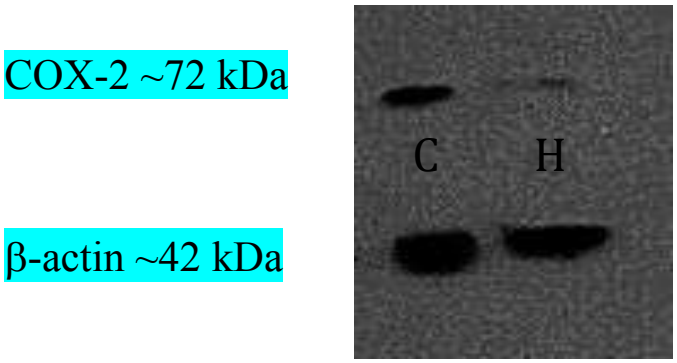
COX-2 ~72 kDa
β-actin ~42 kDa
C
H

Figure 6

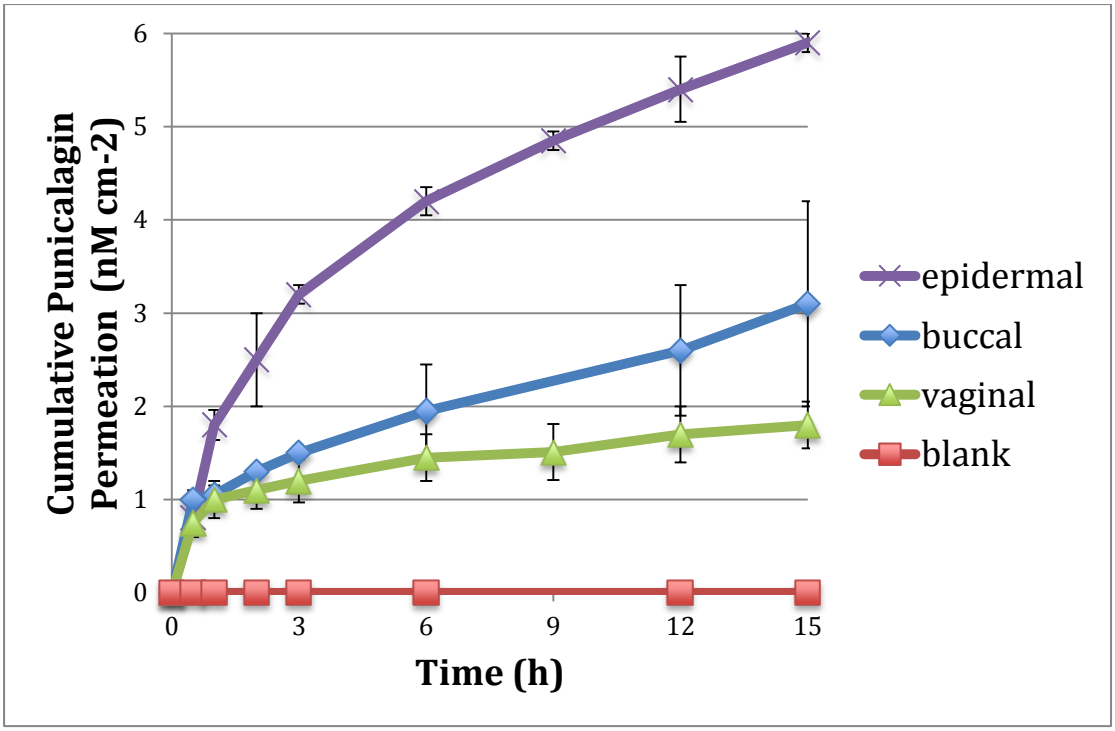
Cumulative Punicalagin Permeation (nM cm-2)
6
5
4
3
2
1
0
0
3
6
9
12
15
Time (h)
epidermal
buccal
vaginal
blank

Figure 7

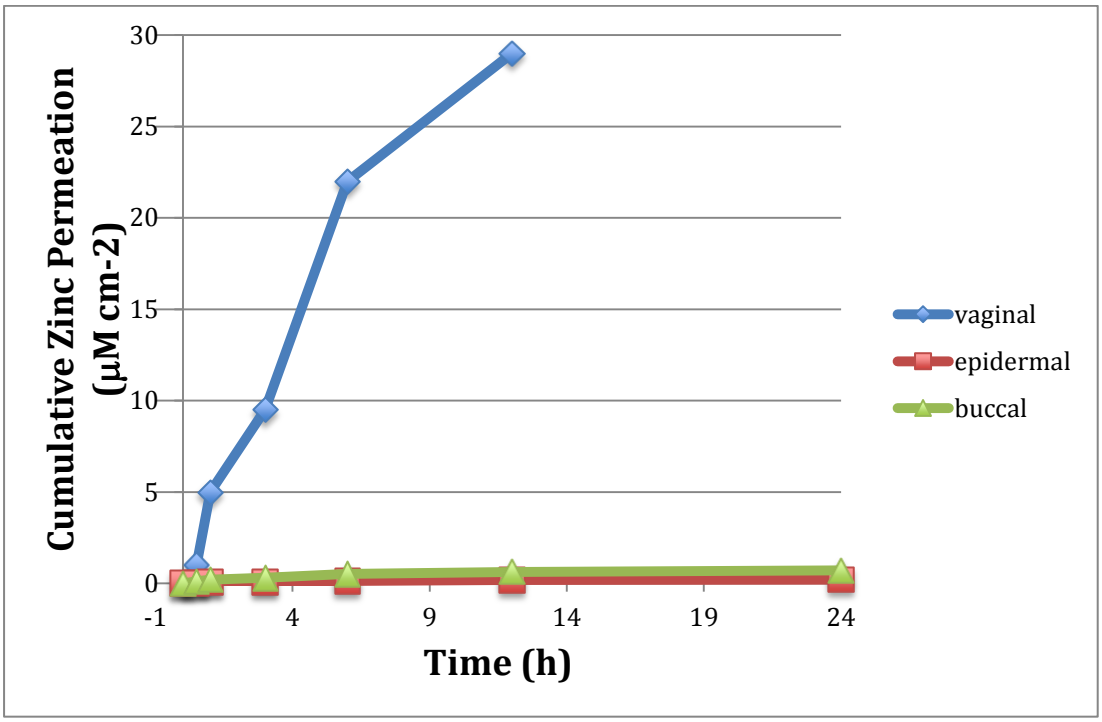
Cumulative Zinc Permeation (µM cm-2)
30
25
20
15
10
5
0
-1
4
9
14
19
24
Time (h)
vaginal
epidermal
buccal

Figure 8

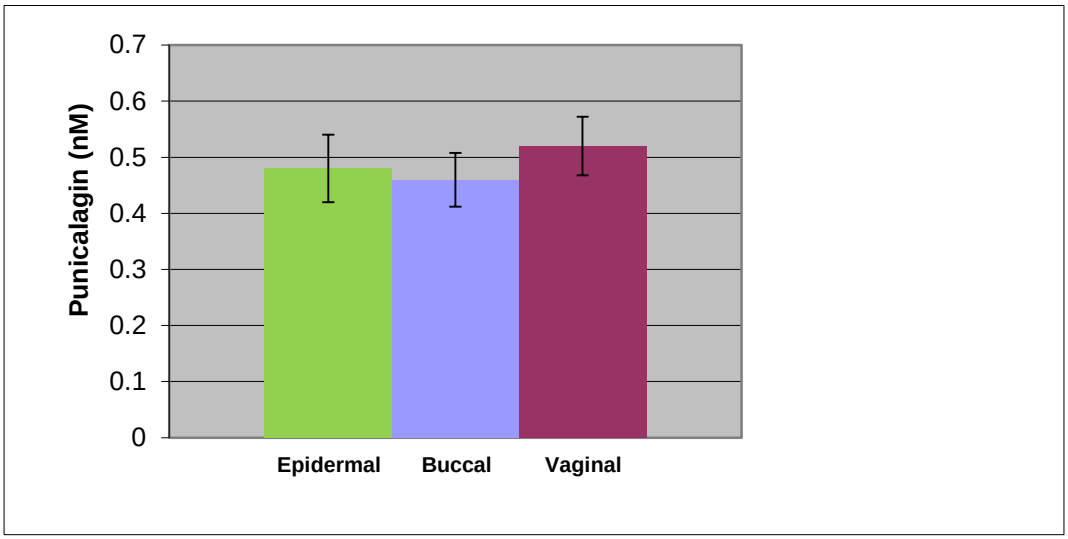
Punicalagin (nM)
0.7
0.6
0.5
0.4
0.3
0.2
0.1
0
Epidermal
Buccal
Vaginal

Figure 9